

PRODUCTION, TUNING AND PROCESSING CHALLENGES OF THE BERLINPRO GUN 1.1 CAVITY*

H.-W. Glock[†], A. Frahm, J. Knobloch, A. Neumann, Helmholtz-Zentrum Berlin für Materialien und Energie, Berlin, Germany

B. Rosin, D. Trompetter, Research Instruments GmbH, Bergisch-Gladbach, Germany

Abstract

For the bERLinPro energy recovery LINAC, HZB is developing a superconducting 1.4-cell electron gun, which, in its final version, is planned to be capable of CW 1.3 GHz operation with 77 pC/bunch. For this purpose a series of three superconducting cavities, denoted as Gun 1.0, Gun 1.1 (both designed for 6 mA) and Gun 2.0 (100 mA) is foreseen. Gun 1.0 now reached rf commissioning status and the Gun 1.1 cavity is completely manufactured. In the paper the chronology of manufacturing, tuning and processing of the Gun 1.1 cavity is described, including details about combined mechanical/electrodynamic simulations, which were performed in order to gain deeper understanding of the cavity's unexpected tuning behavior.

GUN 1.1 CAVITY DESIGN

The design of Gun 1.1 (cf. Fig. 1) as a superconducting 1.3 GHz cavity follows the shape of Gun 1.0 [1, 2], which itself took main concepts and parameters from the HZDR 3.5-cell SRF gun [3], without significant changes. Gun 1.1 serves both as a backup cavity in case of severe failures of Gun 1.0 and as a test bed for the production of Gun 2.0, which in contrast to its predecessors will be equipped with two 115 kW-couplers, needed for 100 mA continuous wave operation. Therefore it is a major aim of the Gun 1.1 production campaign to identify critical manufacturing and processing steps.

The cavity consists of a low energy (“half”) cell of $0.42 \lambda = 48.43$ mm length with a central hole of 11.5 mm diameter in its back wall, which will accommodate the cathode plug. It is directly connected with a full cell of classical TESLA shape [4], i.e. a length of 115.13 mm and an outermost radius of 103.4 mm. Downstream the full cell is delimited by a waist of 35 mm radius followed by a beam pipe of 53 mm radius, thus being able to propagate dipole-type wake power above 1.66 GHz and monopole-types above 2.17 GHz towards a cylindrical dielectric HOM absorber. This beam pipe also accommodates two opposing ports for fundamental power couplers (FPCs) of TTF3-style, modified for 10 kW cw operation. On the upstream side of the cathode plug port a third so-called choke cell is used as a notch filter blocking the coaxial path, consisting of the cathode plug support and the outer wall, for fields with fundamental frequency. The removable cathode plug support is housed in a second

pipe attached in upstream direction to the choke cell. A segmented stiffening ring welded between the half and the full cell stabilizes the iris region between the cavities. A second ring between choke and half cell stiffens both cavity side walls. It has radial connections to an encircling ring that also carries a single bellow convolution, which allows to compress the choke cell from the outside of the helium tank in order to tune it.

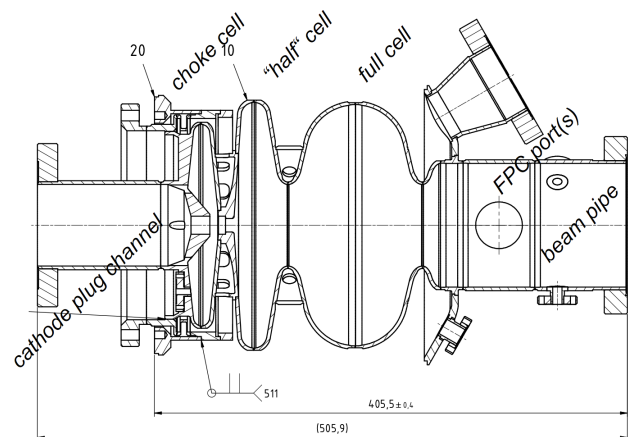


Figure 1: Cross Section of the Gun 1.1 cavity including the LHe-vessel endplate (with He gas chimney and LHe filling port) welded to the beam pipe. The FPCs are oriented perpendicular to the drawing.

CAVITY MANUFACTURING

Research Instruments GmbH produced and processed the Gun 1.1 cavity. Three cups (one spare) of the full cell of TESLA shape and the downstream waist were deep drawn out of 3.2 mm thick niobium sheets (RRR 300). The parts of the half and the choke cell were manufactured by turning from bulk coarse grain niobium (RRR 300). Coupler ports in the beam tube were constructed with a pulling technique. Electron-beam-(EB)-welding was applied after preparing all welds. Stainless steel flanges were directly high-temperature brazed to the niobium pipe sections, which afterwards were connected with the cavity by EB-welding. The shape of the central dumbbell was checked with a Coordinate Measuring Machine (CMM) and revealed an outwards bump of ~ 0.3 mm in the full cell side, most likely introduced by shrinkage from welding the stiffening ring (cf. Fig. 2).

* Work supported by German Bundesministerium für Bildung und Forschung, Land Berlin and grants of the Helmholtz Association

[†] hans.glock@helmholtz-berlin.de

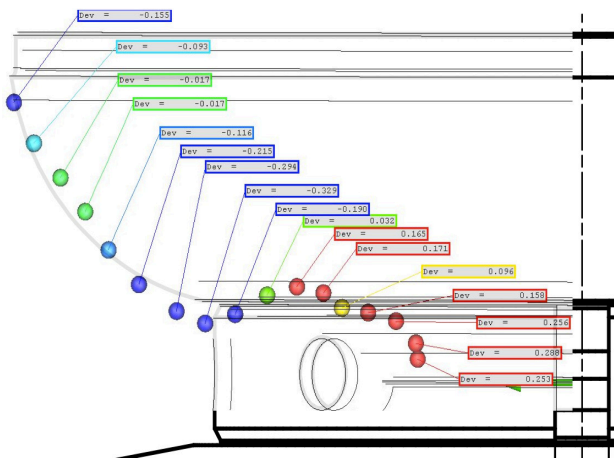


Figure 2: Cross section CMM data for the full cell part of the welded dumbbell, showing a bump of ~0.3 mm close to the stiffening ring weld area (blue dots). Black/grey lines indicate the ideal cell contour and the stiffening ring. Additional material near the iris (red dots) was later removed by grinding.

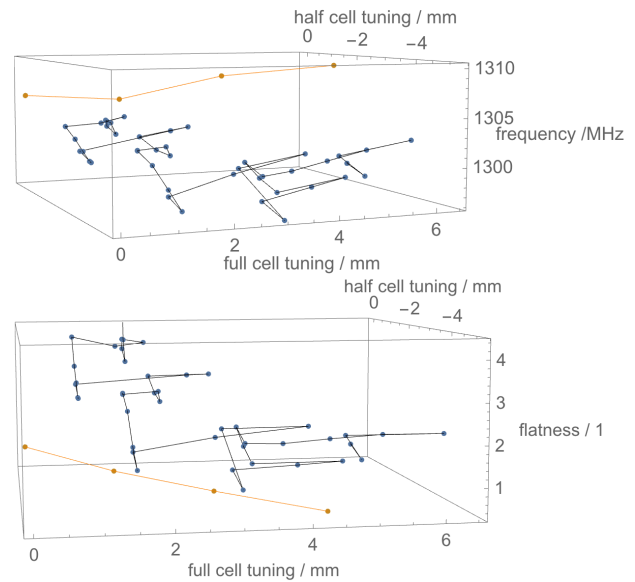


Figure 4: Experimental (blue) and numerical (orange) tuning steps, showing significant differences. “flatness” is defined here as $(E_{half}/E_{full})^2$.

CAVITY TUNING

After welding the cavity was mechanically tuned (Fig. 3) in order to reach same field levels in both cells at a frequency of 1300.600 MHz (as design frequency before chemical etching and further dressing steps). It was not possible to accomplish both requirements simultaneously (Fig. 4). Tuning was stopped at 1300.1 GHz and $(E_{half}/E_{full})^2 = 1.82$ (peak field strengths). In order to identify the most appropriate tuning conditions the shape deformation (Fig. 5) and according field distributions (Fig. 6) were computed in linked mechanical-EM simulations. The material properties of warm niobium used in the simulation of the combined elastic-plastic cavity deformation were taken from [5].

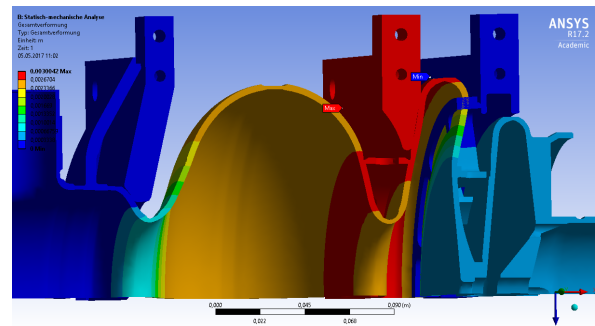


Figure 5: Tuned cavity shape after shifting the central of the three tuning plates 3 mm to the right, calculated by ANSYS [6].

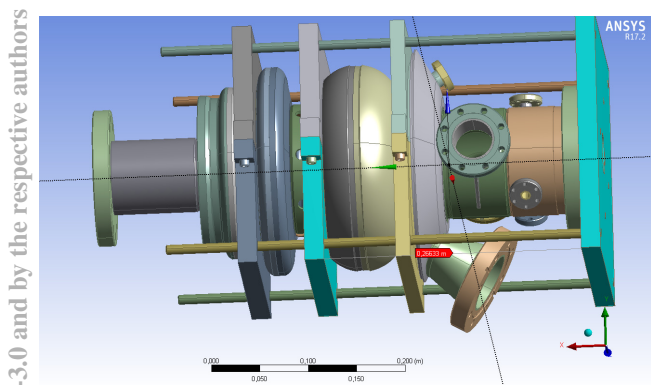


Figure 3: Setup for manual tuning of the Gun 1.1 cavity. Three tuning plates are adjusted by nuts on the four threaded bars. The bottom plate (shown to the right) serves for support purposes only.

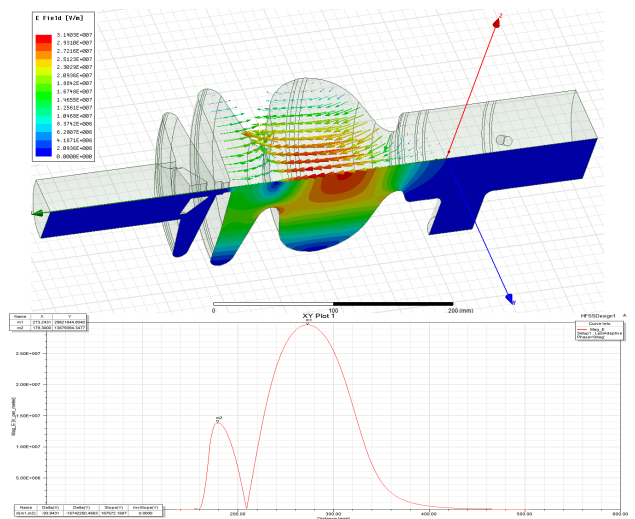


Figure 6: Electrical field in the deformed cavity shape shown in Fig. 5 simulated with ANSYS-HFSS [7]. Absolute E-field values shown in color representation (above) and sampled on the cavity’s axis (below).

This was done both for individual cell tuning, simultaneous full cell stretching/half cell shortening (cf. Fig. 4, orange entries) as approximation to the complex sequence of the actual tuning and also incorporating the weld shrinkage of the stiffening ring. The reasons for the severe differences between simulated and experimental results are still not clear.

BULK CHEMICAL PROCESSING

It is intended to remove in total 200 μm niobium using bulk chemical etching (BCP). Recently two BCP steps were performed and their effect was checked both with ultrasonic (US) wall thickness measurements (using a Panasonic 250LPlus gauge; 6 different lateral and 8 azimuthal positions, 4 to 8 samples per position; averaged 67.5 μm , 13.8 μm) and by weight comparison (202 g, 37 g at 324752 mm^2 resulting in 72.6 μm , 13.3 μm resp.). The field flatness remained practically unaffected in both BCPs; frequency decreased by 670 kHz, 230 kHz resp., corresponding to $\sim 9.6 \text{ kHz}/\mu\text{m}$, $\sim 17.0 \text{ kHz}/\mu\text{m}$.

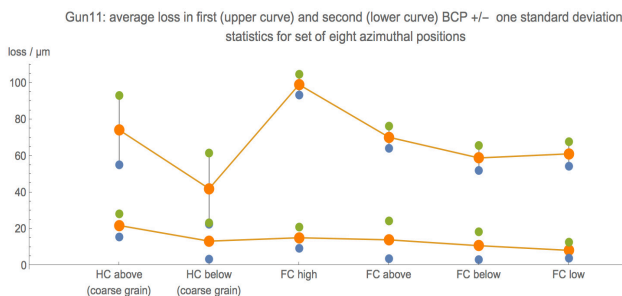


Figure 7: Wall thickness loss in BCP1 (above) and BCP2, averaged over 8 sampling points around the cavity at 6 different longitudinal positions (HC/FC: half/full cell).

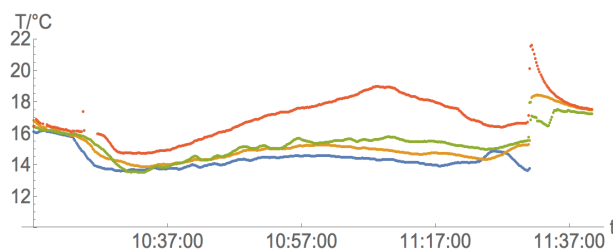


Figure 8: Cavity surface temperatures during BCP2 at the beam pipe transition (blue, disconnected before draining), full cell equator (ocher), full cell stiffening ring (green), half cell equator (red). The temperature rise was stopped with an increased acid exchange rate.

Whereas the full cell experienced a stronger etching in BCP1, the situation was opposite at BCP2. Since the half cell has higher field strengths, this is in agreement with the increased sensitivity seen there. The strongly differing sensitivity indicates differently distributed etching effects in both steps, which is supported by the detailed US measurement results (cf. Fig. 7). The narrow cathode plug hole introduces an issue specific to this cavity shape. Applying a pump-driven acid flow (like it was used e.g.

in the XFEL 9-cell cavities) would enhance the etching rate in the cathode channel in an ungovernable manner. Therefore a magnet mixer was used at BCP1 to introduce fluid movement and acid was fully exchanged thrice after about 20 min each. It turned out that this approach hinders a reliable temperature control, and acid temperatures of up to 34°C were observed in drained acid. At BCP2 a frequent partial acid exchange was successfully used together with surface temperature monitoring (Fig. 8) in order to keep the acid and cavity temperature during the BCP below 20°C. This together with a pre-cooled acid ($\sim 10^\circ\text{C}$) using the ratio 1:1:4 (HF:HNO₃:H₃PO₄; in both BCPs) made the process controllable, even though obviously a temperature and etching gradient from bottom to top developed. Also the final draining process, taking $\sim 150 \text{ s}$, remained difficult. A temperature peak in the (upper) half cell was observed before interior flushing was possible.

During the ultrasonic thickness measurement at the coarse-grain-manufactured half cell the observation of significant jumps in the readouts while crossing a grain boundary was made. This is also reflected in larger standard deviations seen there (cf. Fig. 7) and is interpreted as a sound velocity which depends on the grains' crystal orientations.

CONCLUSIONS AND UPCOMING STEPS

The bERLinPro Gun 1.1 cavity is completely constructed. Both its tuning and BCP turned out to be challenging and optimal tuning was not reached yet. BCP processing and tuning will be continued before the cavity's rf properties including the field profile are going to be tested in cold conditions [8].

REFERENCES

- [1] A. Neumann *et al.*, "Final Acceptance Test of the SRF Photo-Injector Cold String for the bERLinPro Energy Recovery Linac", presented at the 28th Int. Linear Accelerator Conf. (LINAC'16), East Lansing, Michigan, USA, Sep. 2016, paper TUPRC015.
- [2] A. Neumann *et al.*, "First Commissioning of an SRF Photo-Injector Module", presented at the 8th Int. Particle Accelerator Conf. (IPAC'17), Copenhagen, Denmark, May 2016, paper MOPVA049, this conference.
- [3] A. Arnold, J. Teichert: Overview on Superconducting Photoinjectors. *Phys. Rev. ST Accel. Beams*, vol. 14 p. 024801, 2011.
- [4] B. Aune *et al.*, "Superconducting TESLA cavities", *Phys. Rev. ST Accel. Beams*, vol. 3, p. 092001, 2000.
- [5] T.J. Peterson *et al.*, "Pure Niobium as a Pressure Vessel Material", Fermi National Accelerator Laboratory Batavia, Illinois 60510, USA, Rep. FERMILAB-PUB-09-320-TD, 2009.
- [6] ANSYS©, Workbench Vers. 17.2
- [7] ANSYS©-HFSS, Electronic Desktop Vers. 16.2
- [8] A. Velez, A. Frahm, J. Knobloch, A. Neumann, "Developments on a Cold Bead-Pull Test Stand for SRF Cavities", presented at the 17th Int. Conf. on RF Superconductivity (SRF2015), Whistler, BC, Canada, Sep. 2015, paper TUPB078.